Electronic Supplementary Material (ESI) for ChemComm.

Supporting Information

Thermal-Exfoliated Synthesis of N-Rich Carbon-Based Nanosheet from Layered Bulk Crystal of Metal-Hexamine Framework

Experimental Section

Materials

Hexamine (HMT: $C_6H_{12}N_4$) was purchased from Beijing Chemical Works, China. Nickle nitrate hexahydrate ($Ni(NO_3)_2 \cdot 6H_2O$), cobalt nitrate hexahydrate ($Co(NO_3)_2 \cdot 6H_2O$), and cadmium nitrate tetrahydrate ($Cd(NO_3)_2 \cdot 4H_2O$) were purchased from Beijing Tongguang Fine Chemical Industry Research Institute, China. Absolute alcohol (99.7%) was provided by Beijing Chemical works, China. All of the chemicals used were AR grade.

Preparation of samples

Typically, nickel nitrate ($Ni(NO_3) \cdot 6H_2O$) and hexamine (HMT: $C_6H_{12}N_4$) with molar ratio of 1:1 were dissolved in an ethonal solution, respectively. Then, the solution of $Ni(NO_3)_2 \cdot 6H_2O$ was added dropwise to the solution of HMT and immediately the green precipitates were generated, indicating the formation of Ni-HMT metal-HMT frameworks (MHFs). The mixed solution was further keeped still for 24 h for yielding enough Ni-HMT MHFs. Afterwards, the Ni-HMT MHFs were obtained by centrifugation and washed by alcohol several times to remove unreactive sources, and then dried at 80 ^oC overnight in the oven. By replacing the metal source of $Ni(NO_3)_2 \cdot 6H_2O$ with $Co(NO_3)_2 \cdot 6H_2O$ and $Cd(NO_3)_2 \cdot 4H_2O$, respectively, the Co-HMT and Cd-HMT MHFs were obtained. Finally, these MHFs were directly annealed at 800 ^oC for 2 h in Ar atmosphere at a heating rate of 10 ^oC min^{-1} and the corresponding functional 2D nanostructures were obtained.

Characterization

The morphologies and microstructure of the samples were observed by field-emission scanning electron microscopy (FESEM, ZEISS SUPRATM 55) and high resolution transmission electron microscopy (HRTEM, FEI Tecnai G2 F20). The crystal structure was characterized by powder X-ray diffraction (XRD, Rigaku D/max-2500B2+/PC) using Kα radiation (λ=1.5406 Å) over the range 5-90^o (2θ) at room temperature. Elemental analysis (C, H and N) was carried out on a vario EL cube microanalyzer. The specific surface area was measured using the Brunauer-Emmett-Teller (BET) method (ASAP 2020) at 77 K and pore-size distribution (PSD) curve was obtained from N_2 adsorption data using the density functional theory (DFT) method (Micromeritics). Thermogravimetric and differential scanning calorimetry (TG and DSC; Netzsch STA 449C) were performed in the temperature range of 30-800 ^oC with a heating rate of 10 ^oC min^{-1}. The gaseous products evolved upon heating of the samples were studied using a mass spectrometer gas trace A (Fison Instruments) equipped with a quadrupole analyzer (VG analyzer) working in a faraday mode. X-ray photoelectron spectra (XPS) were recorded on a Thermo Electron Corporation ESCALAB 250 XPS spectrometer using a monochromatized Al Kα radiation (1486.6 eV) with 30 eV pass energy in 0.5 eV step over an area of 650 um × 650 um to the sample.

Electrochemical measurements

The electrochemical measurements were tested with a CR2025 coin type cell. Working electrode was prepared by coating the slurry of active materials, acetylene black and sodium carboxymethylcellulose (CMC) at a weight ratio of 80:10:10 on the copper foil, and then drying at 120 ^oC overnight. Pure Na sheet was used as the counter electrode and glass fiber was used as separator. The applied electrolyte was 1 M $NaSO_3CF_3$ dissolved in the diglyme. The cells were assembled in an argon-filled glove box with the concentrations of moisture and oxygen below 1ppm. The galvanostatic charge/discharge cycles of the cells were measured between 0.01 and 2.8 V versus Na/Na^+ at various current densities by using a LAND CT2001 battery tester. Cyclic voltammetry (CV) was recorded at a scan rate of 0.1 mV s^{-1} in voltage range of 0.01-2.8 V on a Zahner Ennium electrochemical workstation.

Table S1. Elemental analysis of the three MHFs.

Samples		C (wt%)	N (wt%)	H (wt %)
Ni-HMT MHFs: $[Ni(NO_3)_2(HMT)(H_2O)_2]_n$	Found:	21.93	24.07	5.08
	Calculated:	20.11	23.41	4.50
Co-HMT MHFs: $[Co(NO_3)_2(HMT)(H_2O)_2]_n$	Found:	21.47	24.60	4.76
	Calculated:	20.10	23.40	4.49
Cd-HMT MHFs: $[Cd(NO_3)_2(HMT)(H_2O)_2]_n$	Found:	18.40	20.41	4.10
	Calculated:	17.46	20.37	3.91

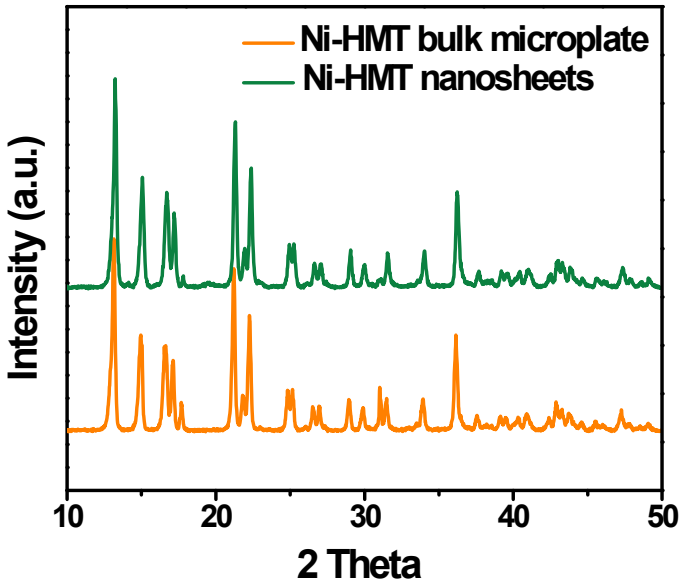

Fig. S1 XRD pattern of the bulk Ni-HMT microplate and Ni-HMT nanosheets obtained by the ultrasonication treatment.

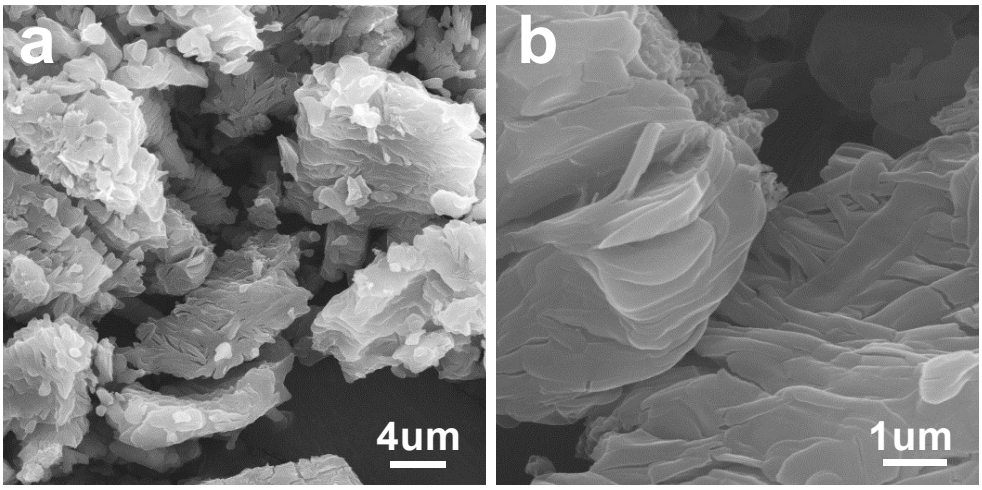

Fig. S2 SEM images of Ni-HMT nanosheets after filtration and drying.

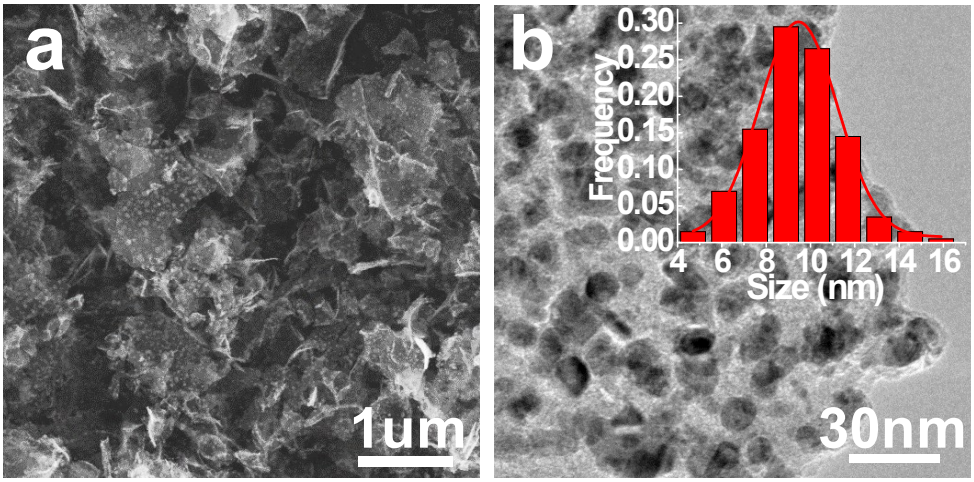

Fig. S3 (a) SEM and (b) TEM images of 2D composite nanosheets by the pyrolysis of bulk Ni-HMT MHFs, and the corresponding size distribution of Ni nanoparticles in the carbon matrix (inset of (b)).

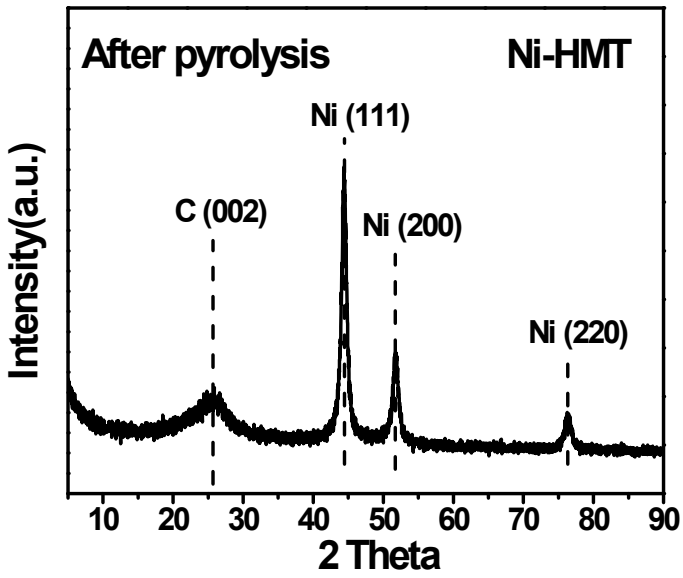

Fig. S4 XRD pattern of Ni-HMT MHFs after pyrolysis.

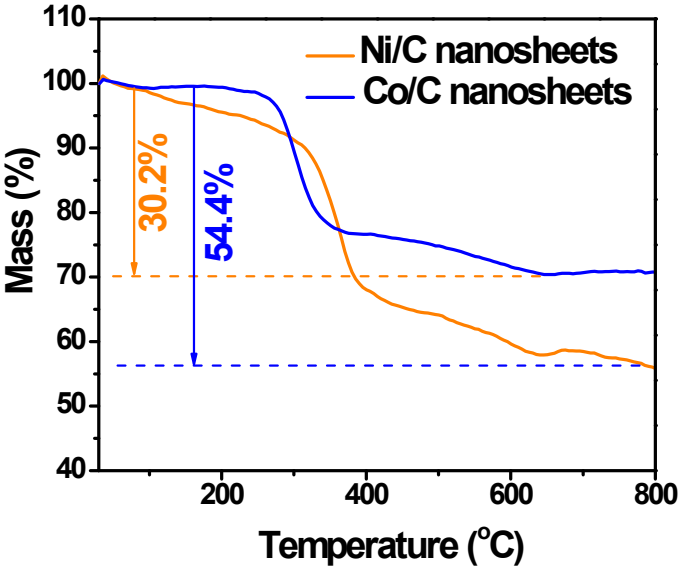

Fig. S5 TG curves of the Ni/C and Co/C nanosheets obtained in air atmosphere from room temperature to 800 °C at a heating rate of 10 °C/min.

The weight changes of Ni is associated with oxidation of Ni to NiO through $2Ni + O_2 = 2NiO$, while Co is associated to $3Co + 2O_2 = Co_3O_4$. Thus, the estimated content of Ni and Co nanoparticles in the Ni/C and Co/C nanosheets is ca. 42.6 and 51.4 wt%.

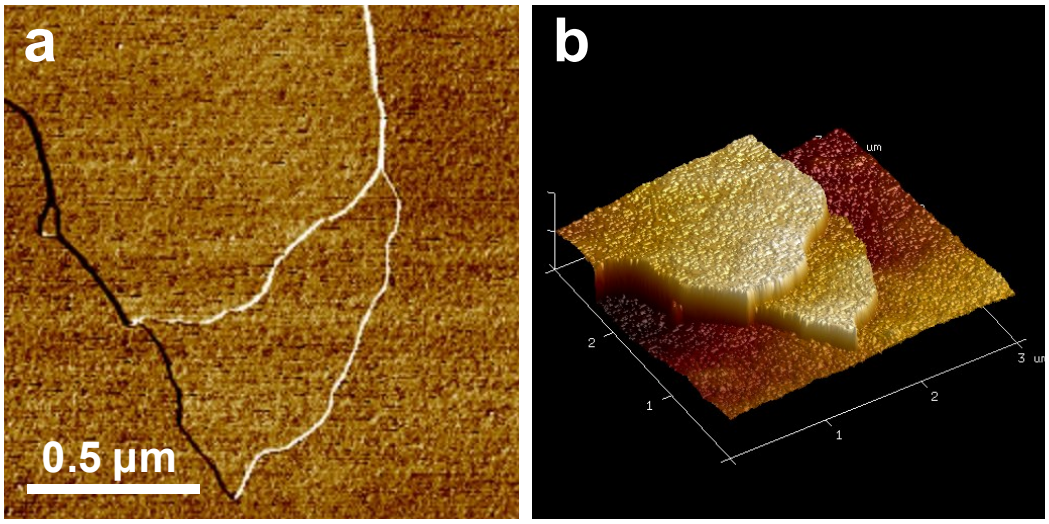

Fig. S6 (a) 2D phase and (b) 3D images fo the 2D carbon-based nanocomposite by the pyrolysis of Ni-HMT MHFs.

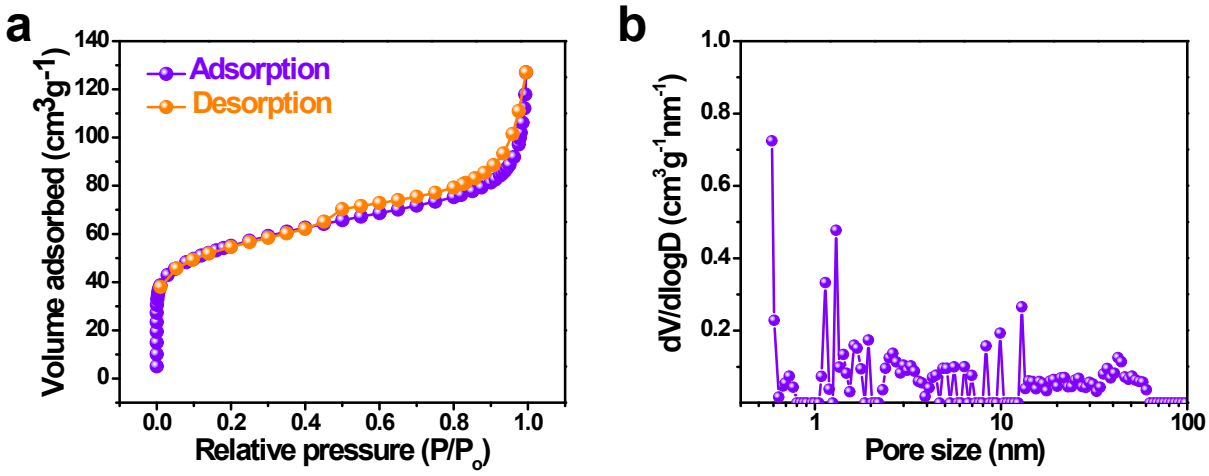

Fig. S7 (a) Nitrogen adsorption-desorption isothermal curve and (b) the corresponding pore-size distribution of the resulting 2D composite nanosheets by the pyrolysis of bulk Ni-HMT MHFs.

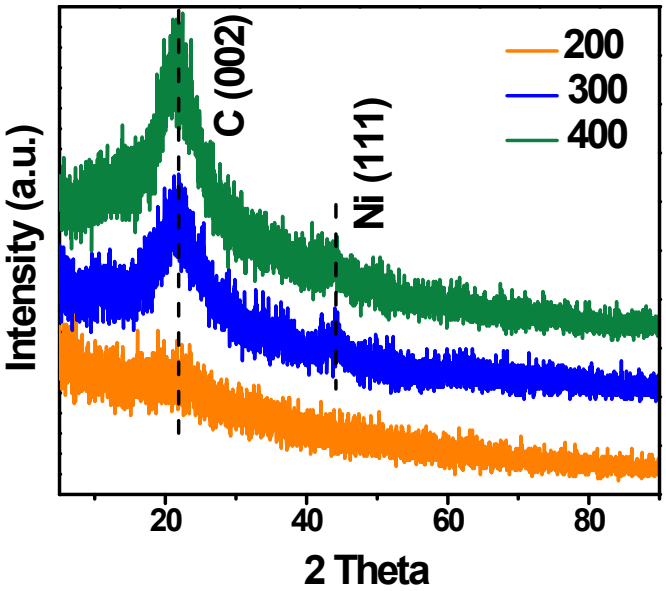

Fig. S8 XRD pattern of the Ni-HMT MHFs annealed at 200, 300, and 400 °C at a heating rate of 10 °C/min.

The XRD patterns of the layered bulk Ni-HMT MHFs treated at 200, 300, and 400 °C are investigated. When treated at 200 °C, the XRD pattern shows that the sample has lost its coordination structure. Simultaneously, a very small broad peak at ca. 23° is observed. This diffraction peak should be assigned to the (002) plane of the graphitic layer structure, indicating that a disordered carbon structure is formed despite the low annealing temperature. With further increasing the annealing temperature to 300 and 400 °C, the (002) peak gradually increases, suggesting the development of the carbon structure. Meanwhile, a small peak at ca. 44° is also present, which is ascribed to the (111) plane of metallic Ni. The results indicate the Ni species have been reduced by the carbon, and the Ni nanoparticles are formed under this temperature.

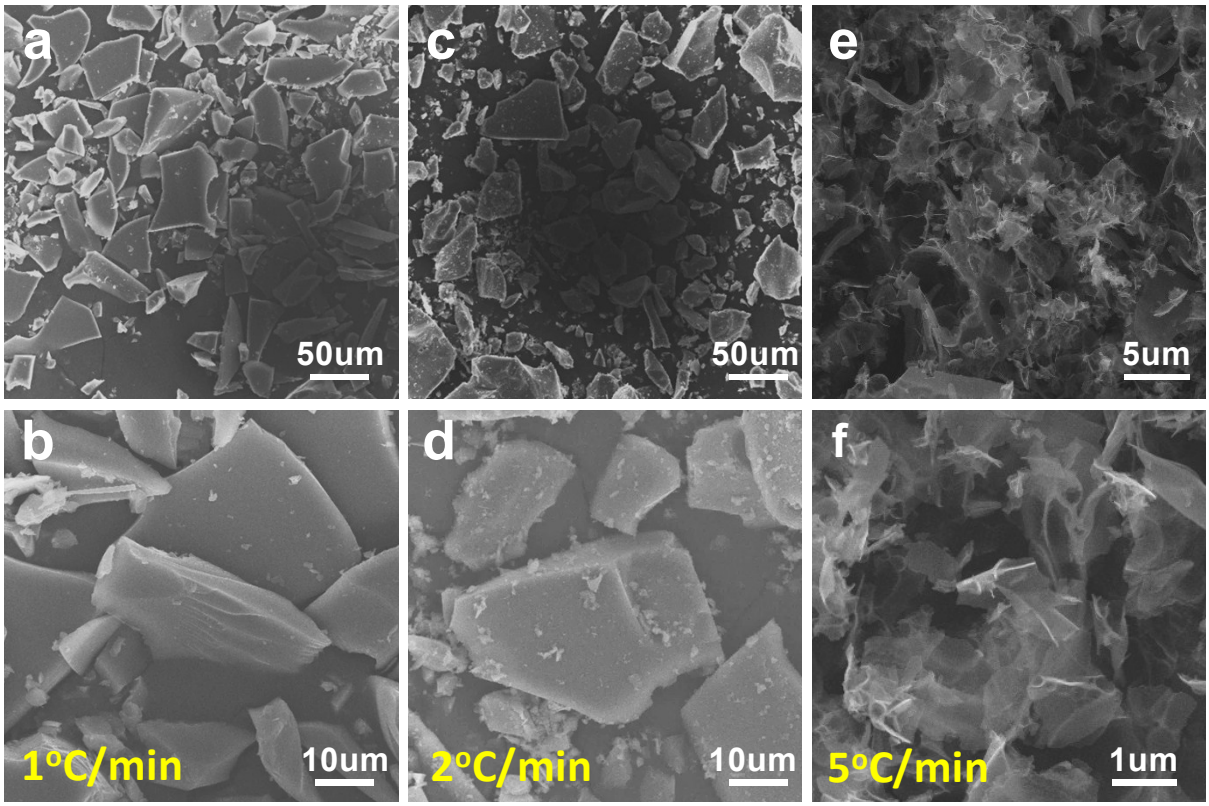

Fig. S9 SEM images of Ni-HMT MHFs pyrolyzed at 600 °C at a heating rate of (a,b) 1, (c,d) 2 and (e,f) 5 °C min^{-1}, respectively.

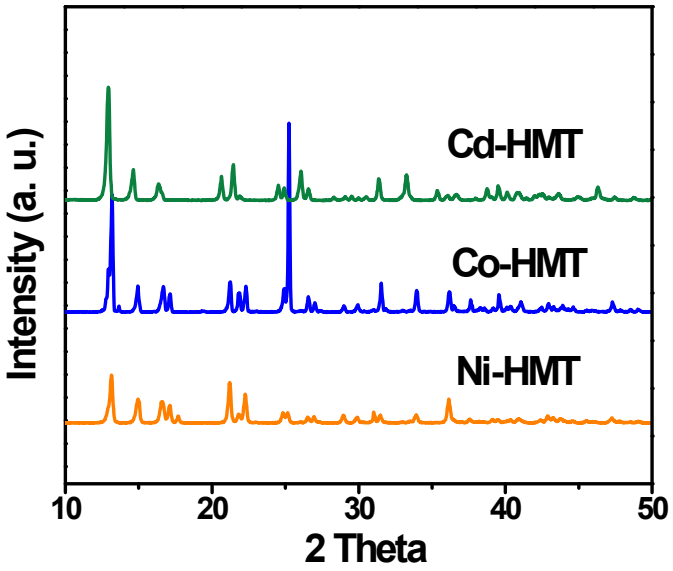

Fig. S10 XRD pattern of Ni-HMT, Co-HMT, and Cd-HMT MHFs.

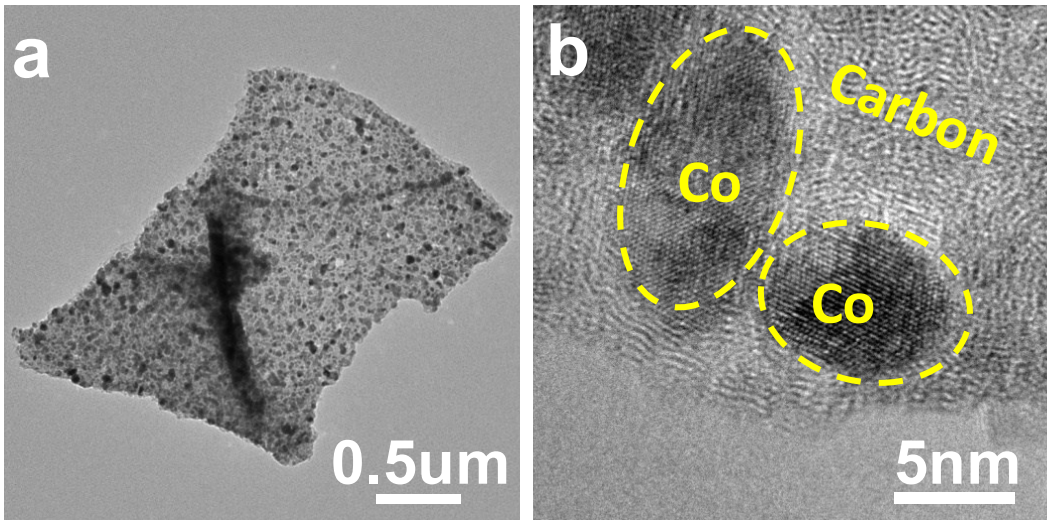

Fig. S11 (a) TEM and (b) HRTEM images of Co-HMT MHFs after pyrolysis.

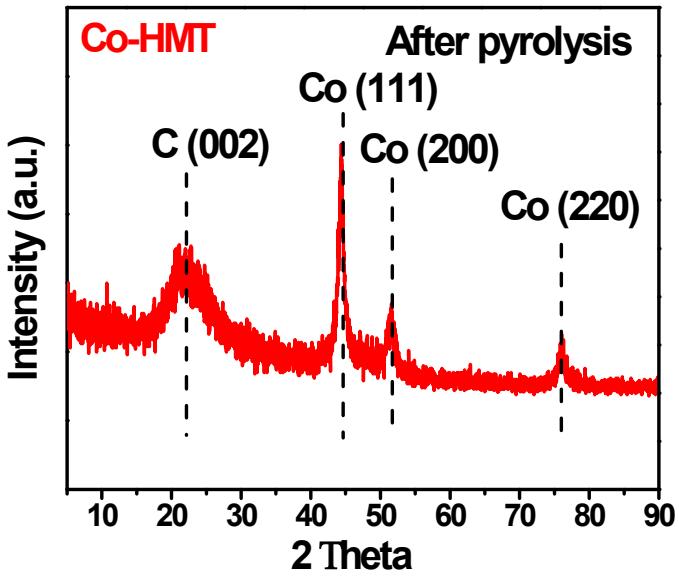

Fig. S12 XRD pattern of Co-HMT MHFs after pyrolysis.

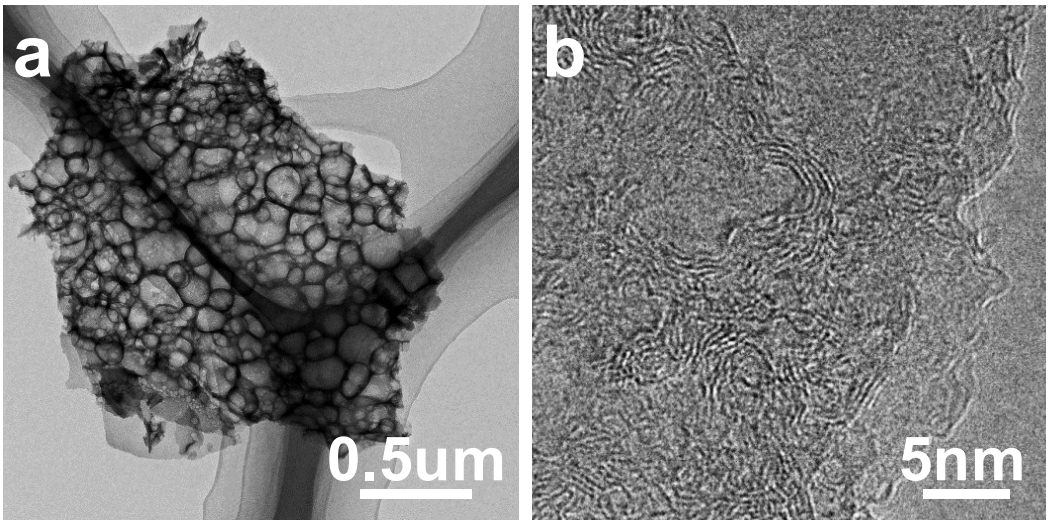

Fig. S13 (a) TEM and (b) HRTEM images of Cd-HMT MHFs after pyrolysis.

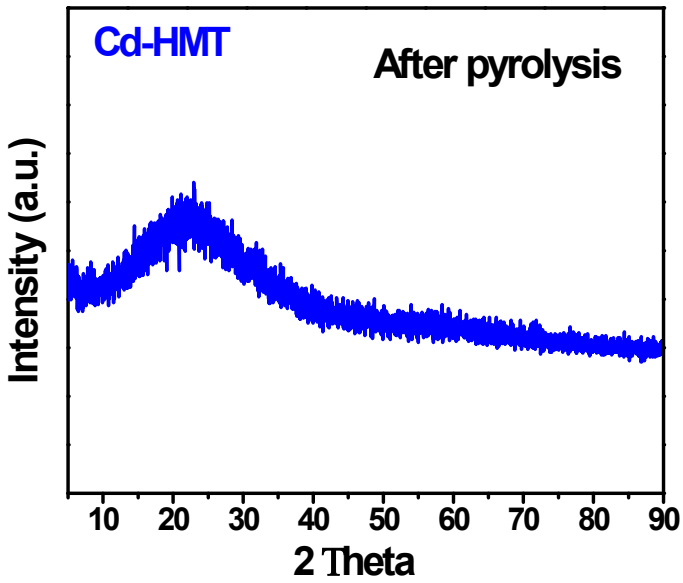

Fig. S14 XRD pattern of Cd-HMT MHFs after pyrolysis.

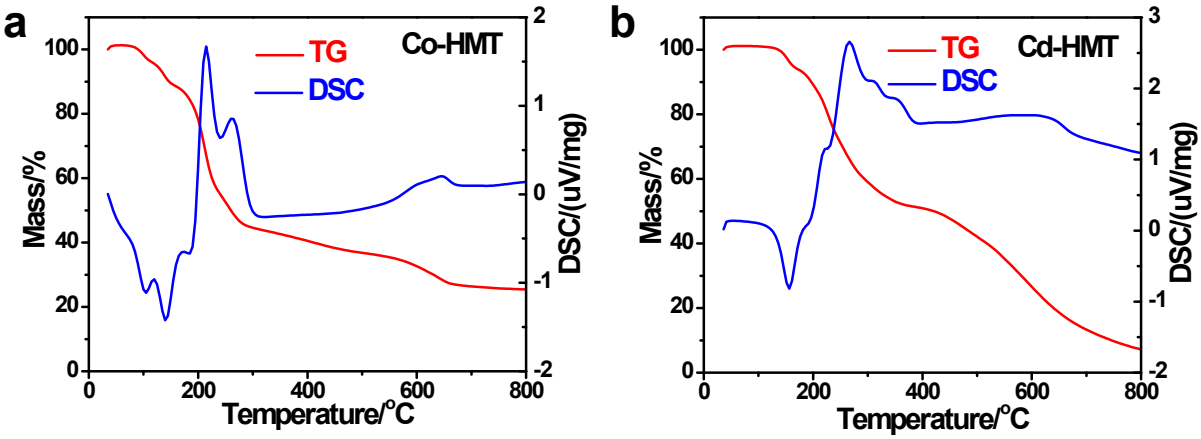

Fig. S15 TG/DSC curves of (a) Co-HMT and (b) Cd-HMT MHFs pyrolyzed under Ar atmosphere.

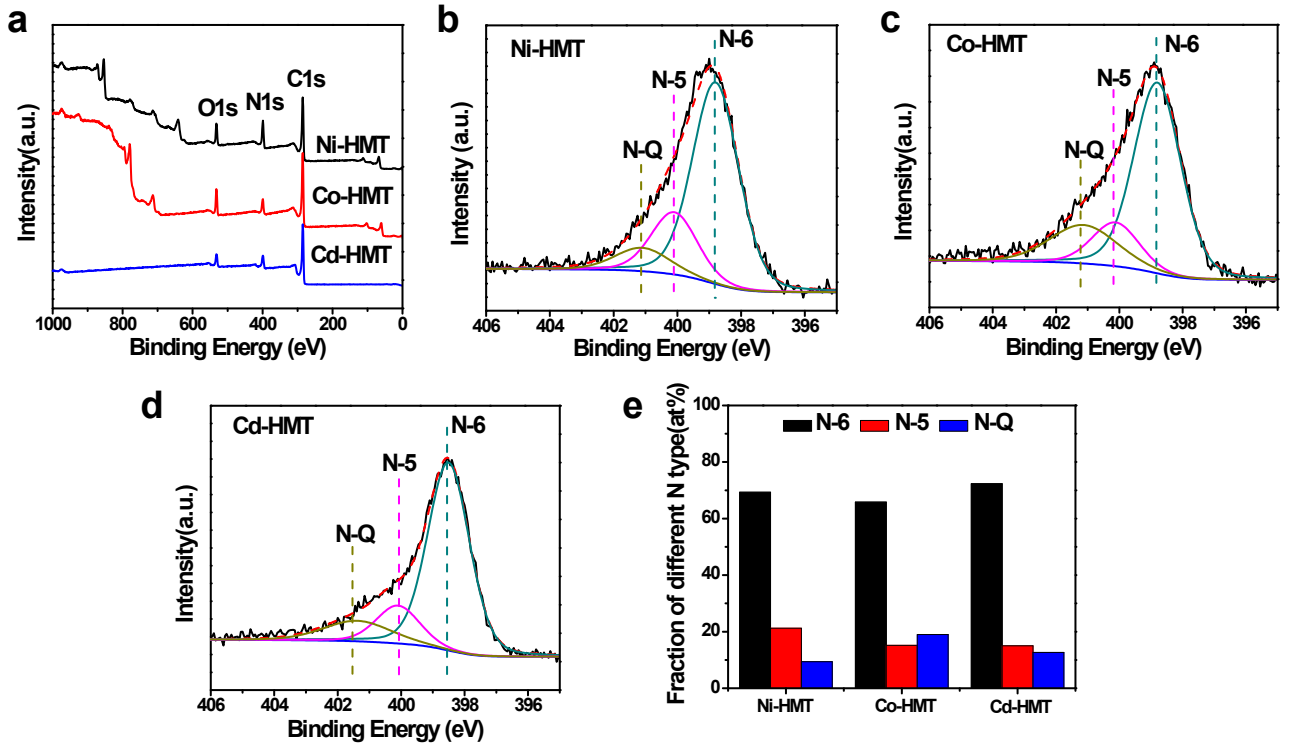

Fig. S16 (a) XPS survey spectra of Ni-HMT, Co-HMT and Cd-HMT MHFs after pyrolysis; high resolution of N 1s spectra of (b) Ni-HMT, (c) Co-HMT and (d) Cd-HMT MHFs after pyrolysis; (e) fraction of different N types in all the three MHFs after pyrolysis.

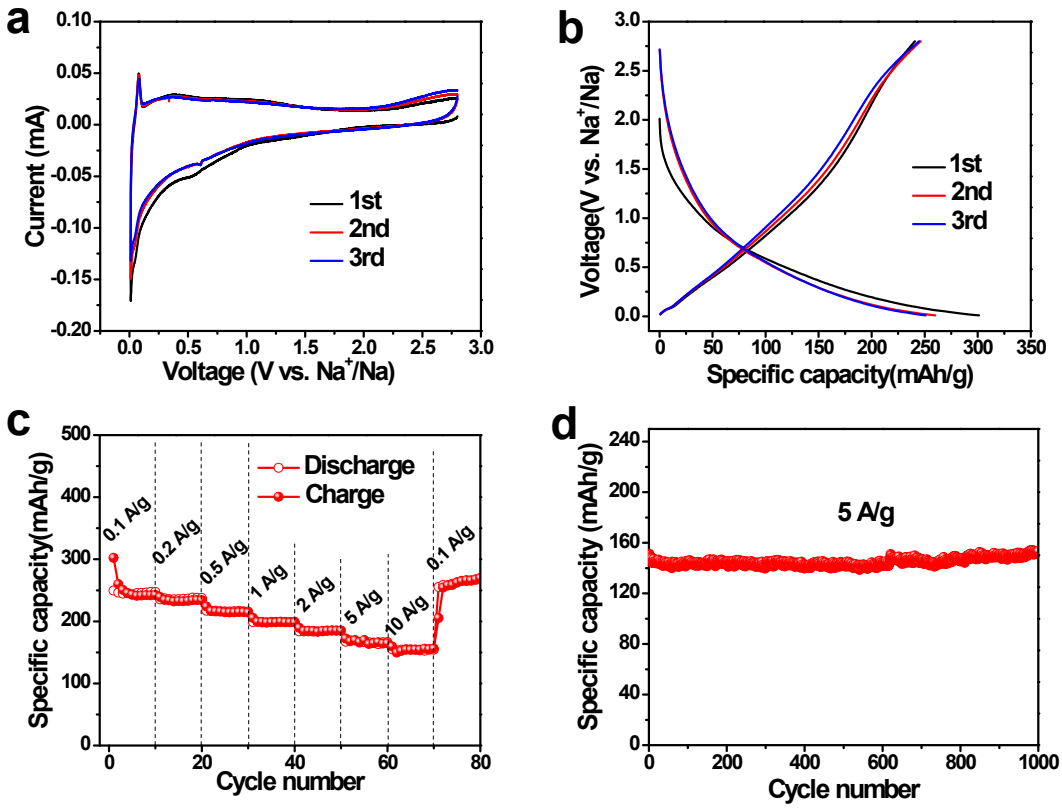

Fig. S17 Electrochemical performance of Cd-HMT MHFs derived N-rich carbon nanosheets. (a) CV curves in a voltage range of 0.01-2.8 V at 0.1 mV s^{-1}; (b) voltage profiles of the first three cycles at a current density of 100 mA g^{-1}; (c) rate performance; (d) long-term cycling performance at the current density of 5 A g^{-1}.